

Los Alamos National Laboratory is operated by the University of California for the United States Department of Energy under contract W-7405-ENG-36

TITLE NUCLEAR EFFECTS ON HEAVY QUARK PRODUCTION, RESULTS FROM FERMILAB
EXPERIMENTS E772 AND E789

AUTHOR(S): M. J. Leitch, D. Alde, H. Baer, J. Boissevain, T. Carey, G. T. Garvey, R. Jeppesen, J. Kapustinsky, A. Klein, D. Lane, C. Lee, J. Lillberg, P. McGaughey, J. M. Moss, J. C. Peng, M. Brooks, G. Brown, D. Isenhowe, M. Sadler, R. Schnathorst, G. Danner, M. Wang, L. Lederman, M. Schub, C. N. Brown, W. E. Cooper, H. Glass, Y. B. Hsiung, C. S. Mishra, K. Gounder, M. R. Adams, G. Gidal, P.-M. Ho, M. Kowitt, K.-B. Luk, D. Pripstein, M. Apolinski, R. Guo, D. M. Kaplan, V. Martin, R. Preston, J. Sa, V. Tatkella, R. Childers, C. Darden, J. Wilson, R. L. McCarthy, Y.-C. Chen, G.-C. Kiang, P.-K. Teng, M. Bartlett, and G. Hoffmann.

SUBMITTED TO: Quark Matter 1991, Gatlinburg, Tennessee, November 11-15, 1991

By accepting of this form the subscriber recognizes that the U.S. Government retains for itself the right to publish or reproduce the submitted form of the submitted or to allow others to do so for U.S. Government purposes.

Use Case: Agency Approval. After they complete that the publisher identify this article is work published under the auspices of the U.S. Department of Energy.

Los Alamos Los Alamos National Laboratory
Los Alamos, New Mexico 87545

This report was prepared as an account of work sponsored by an agency of the United States Government. Neither the United States Government nor any agency thereof nor any of their employees makes any warranty, express or implied, or assumes any legal liability or responsibility for the accuracy, completeness, or usefulness of any information, apparatus, product, or process disclosed or represented, that its use would not infringe privately owned rights. Reference herein to any specific commercial product, process, or service by trade name, trademark, manufacturer, or otherwise does not necessarily constitute or imply its endorsement, recommendation, or favoring by the United States Government or any agency thereof. The views and opinions of authors expressed herein do not necessarily state or reflect those of the United States Government or any agency thereof.

Nuclear Effects on Heavy Quark Production Results from Fermilab Experiments E772 and E789

M. J. Leitch, D. Alde, H. Baer, J. Boissevain, T. Carey, G. T. Garvey,
R. Jeppesen, J. Kapustinsky, A. Klein, D. Lane, C. Lee,
J. Lillberg, P. McGaughey, J. M. Moss, J. C. Peng
Los Alamos National Laboratory, Los Alamos, New Mexico

M. Brooks, G. Brown, D. Isenhower, M. Sadler, R. Schnathorst
Abilene Christian University, Abilene, Texas

G. Danner, M. Wang,
Case Western Reserve, Cleveland, Ohio

L. Lederman, M. Schub
University of Chicago, Chicago, Illinois

C. N. Brown, W. E. Cooper, H. Glass, Y. B. Hsiung,
C. S. Mishra, K. Gounder
Fermilab, Batavia, Illinois

M. R. Adams
University of Illinois at Chicago, Chicago, Illinois
G. Gidal, P.-M. Ho, M. Kowitt, K.-B. Luk, D. Pripstein
Lawrence Berkeley Laboratory, Berkeley, California

M. Apolinski, R. Guo, D. M. Kaplan, V. Martin,
R. Preston, J. Sa, V. Tanikella
Northern Illinois University, DeKalb, Illinois

R. Childers, C. Darden, J. Wilson
University of South Carolina, Columbia, South Carolina

R. L. McCarthy,
SUNY at Stony Brook, Stony Brook, New York

Y.-C. Chen, G.-C. Kiang, P.-K. Teng
Institute of Physics, Academia Sinica, Taipei, Taiwan

and

M. Bartlett, G. Hoffmann,
University of Texas, Austin, Texas
(E772 and E789 Collaborations)

I. Introduction

Fermilab Experiments E772 and E789 are fixed target experiments with 800 GeV protons incident on nuclear targets corresponding to a center-of-mass energy of $\sqrt{s} \sim 39$ GeV. Measurements are made with a pair spectrometer which has a solid angle of a few percent and operates at high luminosity with up to $\sim 10^{12}$ (E772) or $\sim 10^{11}$ (E789) protons/spill. Our experimental program explores several types of nuclear medium effects: the modification of quark and gluon structure functions by the nucleus, effects on the production of vector mesons (e.g. J/ψ and Υ), and effects on the production of D mesons. The latter is accomplished with the use of a new silicon vertex detector. E789 also looks at the decays of B mesons including the decay to J/ψ and searches for the decays to two-charged particles (e.g. $B \rightarrow h^+ h^-$) but I will not discuss this part of our program in this talk.

II. Structure Functions

The dominant processes involved in Drell-Yan (DY) and in vector meson production are shown in Fig. 1. These processes provide information on the structure functions of the struck partons, which give the probability for the parton involved to have a certain fraction, x , of the nucleon momentum. The DY process involves the annihilation of a proton beam quark (anti-quark) with a target anti-quark (quark). Unlike deep inelastic lepton scattering where one is sensitive to both the target quark and anti-quark structure functions DY is primarily sensitive to the target anti-quark structure function in the kinematic region of our experiment. For resonance production (J/ψ , ψ' , and Υ) the dominant mechanism is that of gluon-gluon fusion which involves the product of the beam and target structure functions.

The basic physical ideas behind a number of the common theoretical models for the modification of structure functions by the nucleus can be illustrated in fairly simple terms. In the discussion that follows I will look at the ratio of structure functions between a heavy nucleus and deuterium, $R(A/D)$, versus target quark momentum fraction, x_2 . A constant value of one corresponds to no nuclear effect. x_1 (x_2) represents the beam(target) parton momentum fraction and $x_F = x_1 - x_2$.

i) Nuclear binding and Fermi motion¹⁻³:

In principle nuclear binding will produce excess pions in the nucleus which would carry off some of the nucleon momentum and thus cause a reduction in the apparent momentum fraction of the quarks in the nucleon. This produces an effect in the ratio as shown in Fig. 2a. However the pion has a valence anti-quark (which has a fairly hard momentum fraction) while the nucleon has only soft (sea) anti-quarks. Thus the excess pions in a heavy nucleus might be expected to cause an increase of the ratio at large x for the Drell-Yan process which is primarily sensitive to the anti-quarks (Fig. 2b).

At large x the nucleon structure function becomes relatively small. However Fermi motion in a nucleus can spread this distribution to produce a finite population near $x = 1$. A ratio such as shown in Fig. 2c results.

ii) Rescaling⁴⁻⁶:

The rescaling model in it's simplest form is a phenomenological relationship where the structure function in a nucleus is equal to the unmodified nucleon structure function evaluated at a larger Q^2 , i.e.

$$F_2^A(x, Q^2) = F_2^N(x', Q^2)$$

With $\gamma = 2$ reasonably good agreement is obtained with the DIS data. This is equivalent to a $\sim 15\%$ increase in the QCD confinement scale⁶. A larger size scale corresponds to a lower momentum. Thus the momentum fraction of the quark is "softened" and there is

a loss of valence quark momentum. The resulting dependence of the ratio will then look something like Fig. 2d. One simple model which produces such an increase of scale is that of Close, Jaffee, Roberts, and Ross⁶ where they introduce an increased confinement scale that is proportional to the overlap of nucleons. The nucleon overlap is calculated using different correlation functions and single-particle densities. They then assume that when two nucleons overlap their quarks propagate over a larger spatial domain resulting in a corresponding increase in scale.

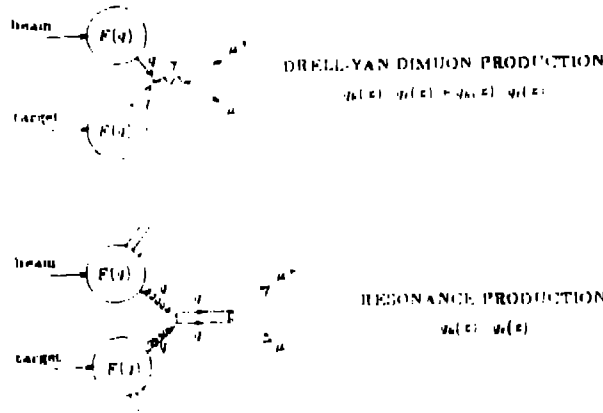


Fig. 1. The Drell-Yan and gluon-gluon fusion processes.

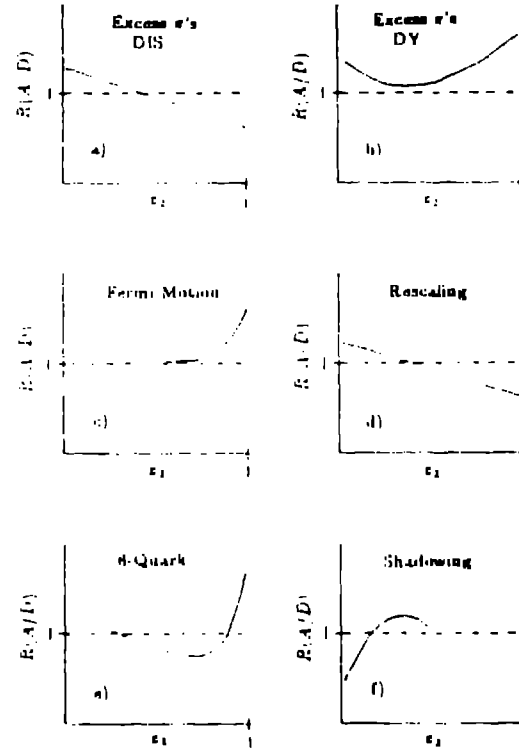


Fig. 2. Schematic expectations for different EMC models as labeled.

iii) Multi-quark clusters^{7,8}:

Multi-quark cluster models obtain a larger length scale by assuming a probability ($\sim 16 - 30\%$) for nucleons in a nucleus to form six or more quark clusters. This should produce the same kind of dependence on x in the ratio as does rescaling. However, as shown in Fig. 2e, a relative enhancement near $x = 1$ should also be produced since one quark can assume the momentum of a single nucleon or more.

iv) Shadowing:

Shadowing refers to the depletion of low-momentum partons (quarks and gluons) in the region of $x < 0.1$. Classically the name "shadowing" refers to the phenomena where a nuclear cross section increases with A^α where α is less than one. This would occur, e.g. in photon reactions, when the interior of the nucleus was shadowed by a front surface which strongly interacts with the probe or is black. However in the discussion of structure functions the term is used to refer only to the low x region where the cross section per nucleon decreases faster than A (i.e. $\alpha < 1$). One simple explanation of this phenomenon is that the low x partons have a large spatial extent and therefore overlap and interact causing a redistribution of their momenta. The typical effect of shadowing on the ratio is shown in Fig. 2f where there is a slight enhancement or "anti-shadowing" just above $x = 0.1$ in addition to the depletion below $x = 0.1$. Another recent explanation of the shadowing phenomena from Brodsky and Lu⁹ involves a detailed parton multiple scattering picture and produces similar effects in the ratio.

III. Reaction Dynamics

A number of reaction dynamics effects must be considered when studying these high-energy reactions.¹¹ Some of these are depicted in cartoon form in Fig. 3. For the Drell-Yan process we expect to see some initial-state multiple scattering and energy loss effects which will broaden the transverse momentum, p_T , of the dimuon pair and shift the effective x_F of the interaction. In the case of resonance production, e.g. J/ψ production, other final-state effects enter and the situation is more complicated. A $c\bar{c}$ or pre- J/ψ pair is formed in an almost point-like interaction and then must spread out for a considerable distance (e.g. 5-10 nuclear radii) at which it achieves a separation distance corresponding to the J/ψ diameter and it hadronizes. The actual distance of course depends on both the x_F at which it is produced and differs according to what meson is produced. In addition a splash of low-energy π 's, ρ 's, and nucleons is created by the incident beam quarks. Some of these can be co-moving with the pre- J/ψ , i.e. have small relative velocity with respect to the pre- J/ψ . The pre- J/ψ can then be multiple scattered or can be dissociated by the co-movers, e.g. $J/\psi + N \rightarrow L + \bar{D} + X$. The pre- J/ψ can also be dissociated by the nuclear medium directly, however since the co-movers can continue to interact well outside of the nuclear volume they may in principle have a more important effect.

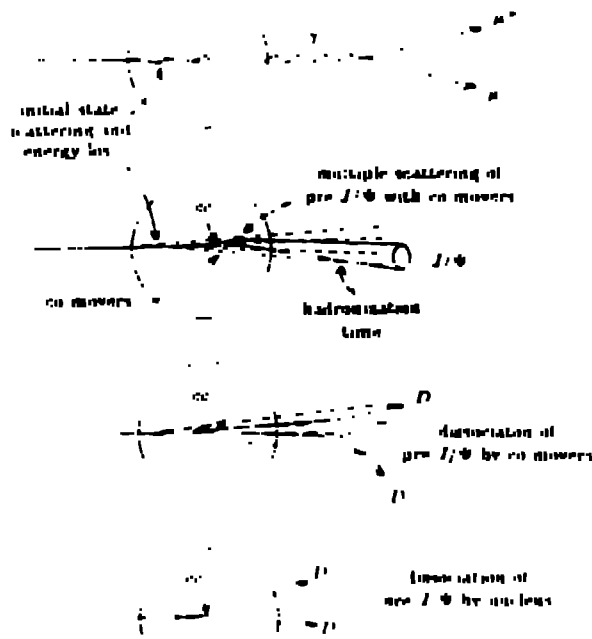


Fig. 3. Some of the reaction dynamics effects for Drell-Yan and J/ψ production in nuclei.

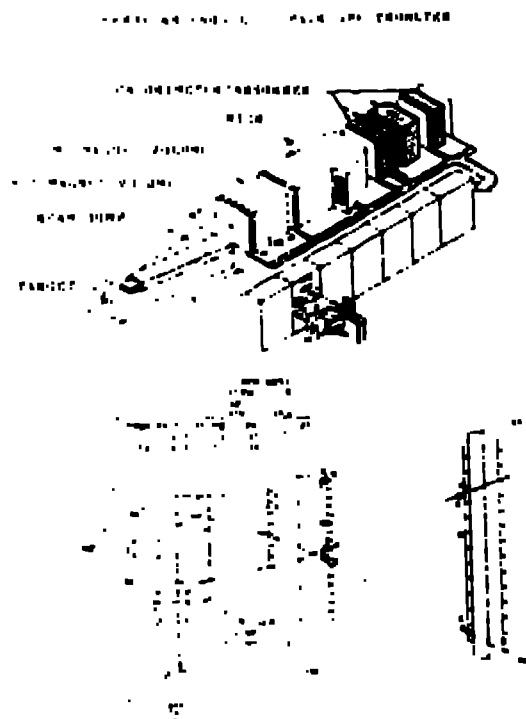


Fig. 4. The Fermilab E605-E772 pair spectrometer with a reconstructed event shown in the bottom panel.

Several other complications are worth mentioning. First, the actual gluon-gluon fusion process will involve an extra soft gluon in the final state which will cause a slight "smearing out" of the kinematic relationships between the detected particles and the actual gluons involved. Second, for J/ψ production it is likely that perhaps one half of the J/ψ 's produced are fed from γ states. Finally, there is the model of Brodsky et al.¹² which involves an intrinsic charm component in the incident proton. In this model the non-intrinsic charm components of the incident proton are large in size and

are stripped off on the black nuclear surface according to $A^{2/3}$. This leaves a spatially small $c\bar{c}$ which can then readily penetrate the nucleus and become a J/ψ . An analogous process involving intrinsic beauty could contribute to Υ production. These processes could then cause an $A^{2/3}$ dependence in the ratio at large x_F where they would be expected to provide the dominant contribution to the cross section.

IV. Experiment E772¹³

Fermilab E772 measures the A -dependence of the Drell-Yan process and of resonance production at a c.m. energy of ~ 39 GeV by colliding 800 GeV protons with fixed nuclear targets. By measuring the momenta of the muon pair one can then calculate the beam parton and target parton momentum fractions. For the DY process the differential cross section is related to the structure functions by,

$$\frac{d^2\sigma}{dM dx} = K(Q^2, x_F) \frac{8\pi\alpha^2}{9M^3} \frac{x_1 x_2}{x_1 + x_2} \sum e_i^2 \{F_i^1(x_1) \bar{F}_i^2(x_2) + \bar{F}_i^1(x_1) F_i^2(x_2)\},$$

where $x_1(x_2)$ is the beam (target) quark momentum fraction and $F_i^j(\bar{F}_i^j)$ is the quark (anti-quark) structure function with $j = 1, 2$ corresponding to beam, target, and where the sum over i is over types of quarks. The K -factor in front of this expression represents QCD corrections and is ~ 2 ; however the cross-section factorizes¹⁴ so that this factor is constant over the quark momentum fraction. Thus in our experiment, which for the DY process involves almost exclusively the product of the beam quark and target anti-quark structure functions, the cross section is a direct measurement of this structure function product.

The detector used at Fermilab for E772 is shown in Fig. 4. Drell-Yan cross sections in the $3 \leq M_{\mu^+\mu^-} \leq 16$ GeV region are only a few $pb's/GeV$. However this detector has good acceptance for $\mu^+\mu^-$ pairs ($\approx 5\%$) and can handle a very high rate of protons on target (up to $2 \times 10^{12}/\text{spill}$). The portion of the 800 GeV protons which does not interact in the target is absorbed in the beam dump contained within the first magnet. Produced muon pairs are analyzed by two large magnets with a total p_T -kick of about 6 GeV. A copper/carbon/polyethylene absorber near the rear of the first magnet protects the detectors downstream of the first magnet from low energy particles from the target, beam dump, or magnet walls. Several sets of scintillator hodoscopes and wire chamber or drift chamber planes throughout the rest of the detector accurately determine the momenta of the two muons. A calorimeter and a thick absorber assure that only muons penetrate through to the rearmost planes of detectors which then provide a clear muon identification. The measured momenta and the track angles are then used to reconstruct physics quantities. The resulting mass spectrum is shown in Fig. 5. In addition to the Drell-Yan continuum we also see the J/ψ and ψ' peaks near the lower end of the acceptance and several Υ peaks near the high end. For the Drell-Yan results that will be shown throughout the rest of this paper only the cross-hatched areas ($4 < M < 9$ and $M > 11$ GeV) will be used in order to avoid systematic errors related to peak determination for the resonances. The data obtained for the three settings of the magnets is summarized in Table I, as are the statistical uncertainties for the Drell-Yan data obtained for the different x_2 bins covered by the experiment. Of the 670k total dimuon events there are 450k Drell-Yan pairs, 100k J/ψ 's, 12k ψ' 's, and 27k Υ 's. Careful and redundant beam monitoring, target thickness determinations, and frequent target interchange resulted in a total systematic error of less than 2%.

V. A -dependence of Drell-Yan

The Drell-Yan results in terms of the ratio between heavy and light target versus $x_1(x_2)$ are shown in Fig. 6. If there were no modification of the nucleon anti-quark structure function by the nuclear medium the data would fall on a ratio of one. In fact, the data are consistent with one except in the low x_1 shadowing region where a significant depletion can be seen as the nuclear mass gets large (i.e. for $W < 2M$). We have plotted the EMC result¹⁵ for $Su-2H$ with our $W < 2H$ result in the bottom right

TABLE I - E772 DATA SUMMARY

| Magnet Setting | $\langle M(\mu^+\mu^-) \rangle$ | Targets | Proton Flux | Dimuon Events |
|----------------|---------------------------------|-----------------------|----------------------|---------------|
| Low mass | 4.8 GeV | Fe/Ca/LD ₂ | 6×10^{15} | 170 k |
| | | W/C/LD ₂ | 2×10^{15} | 70 k |
| Medium mass | 6.5 GeV | Fe/Ca/LD ₂ | 2.4×10^{16} | 280 k |
| | | W/C/LD ₂ | 0.9×10^{16} | 110 k |
| High mass | 9.1 GeV | Fe/Ca/LD ₂ | 1.5×10^{16} | 40 k |
| TOTAL | | | 5.6×10^{16} | 670 k |

Statistical Errors in Drell-Yan Cross Section Ratios for Various x_2 Bins ($x_F > 0$)

| Target | 0 - 0.05 | 0.05 - 0.1 | 0.1 - 0.15 | 0.15 - 0.2 | 0.2 - 0.25 | 0.25 - 0.3 |
|--------|----------|------------|------------|------------|------------|------------|
| Ca, Fe | 1% | < 1% | 1% | 2% | 5% | 12% |
| C, W | 2% | 1% | 2% | 4% | 10% | 24% |

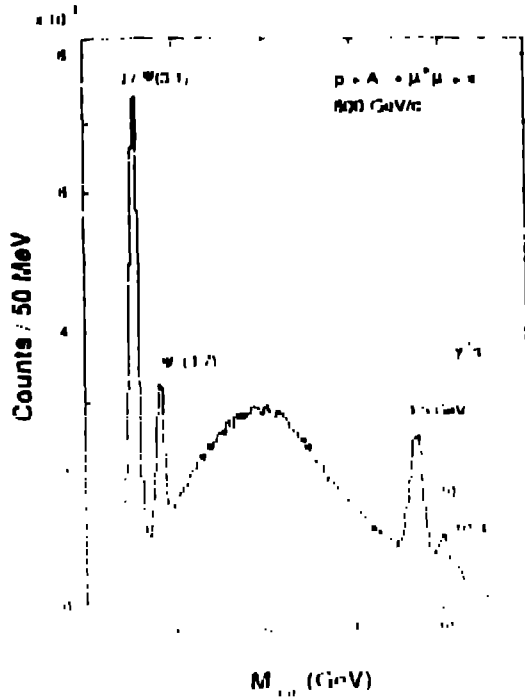


Fig. 5. Muon pair mass spectra obtained in E772 for 800 GeV protons on deuterium.

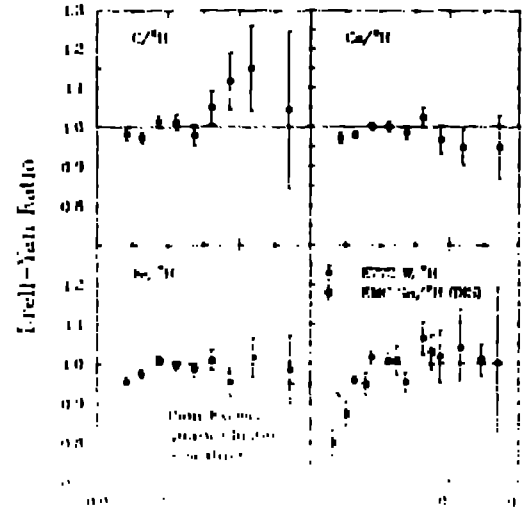


Fig. 6. Target momentum fraction (x_2) dependence of the Drell-Yan dimuon yield per nucleon for positive x_F . The curves shown for Fe/ 2H are predictions of various models as described in the text. Also shown are the deep inelastic scattering data for Sn/ 2H from the EMC group.¹⁵

panel. The depletion in the shadowing region for the EMC data is apparently stronger than that seen in our data. However it is difficult to make a direct comparison since this EMC data in the shadowing region corresponds to Q^2 's between 4 and 14 GeV^2 while the E772 data corresponds to Q^2 above 16 GeV^2 . For our $\text{Fe}/^2\text{H}$ ratio we compare with specific model calculations obtained from Hwang, Moss, and Peng.¹⁶ The pion excess model uses a $g'_0 = 0.6$ and badly misses the data. The quark cluster calculation which follows the model of Carlson and Havens⁷ and uses a 6-quark cluster probability of 15% also badly misses the data. Only the rescaling model agrees at all with the data. The disagreement for $x \leq 0.1$ can presumably be fixed by adding in a depletion due to shadowing.

VI. A-dependence of Resonance Production

The mass dependence of the ratio of integrated cross sections (summed over x_f and p_T) for resonance production from E772 is shown in Fig. 7. Also shown for comparison is the Drell-Yan data whose total cross section has no mass dependence and lies on the horizontal line at $R = 1$. All the resonances shown have a strong A-dependence with the lighter resonances (J/ψ and ψ') having the strongest suppression with mass. A simple fit of the form $R = A^\alpha$ has been done to the resonances (with the J/ψ and ψ' fit together and the Υ 's fit together). The resulting α 's are 0.96 for the Υ and 0.92 for the J/ψ and ψ' . Although some of this A dependence could be caused by a modification of the gluon structure function in nuclei it seems likely that most of it caused by nuclear effects in the final-state such as those described in Section III.

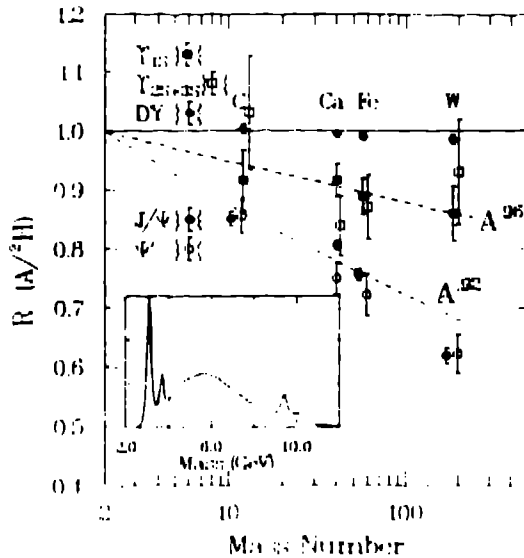


Fig. 7. Nuclear-mass dependence of resonance production compared to Drell-Yan for the ratio from E772. For the Υ -1S and -2S and for the J/ψ + ψ' results of A^α fits are shown.

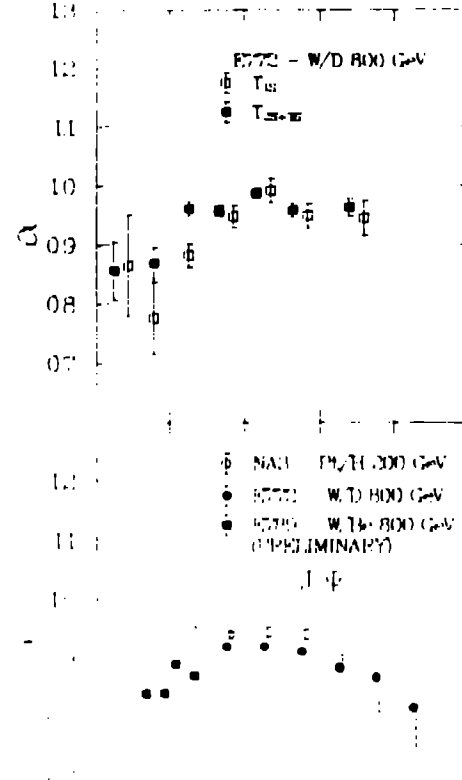


Fig. 8. x_F dependence for J/ψ and Υ production from E772 with preliminary data for small and negative x_F from E789.

The x_F dependence of α for resonance production from E772 and E789 is shown in Fig. 8. New preliminary data from our 1990 E789 test run extend the published E772 data for the J/ψ to values of x_F of zero and below. Both the J/ψ and the Υ 's have a

stronger suppression at $x_F \approx 0$ and below. This suppression, as suggested by Brodsky and Vogt,¹⁷ may be caused by the comovers which might be expected to have a larger overlap with a pre-meson when it is moving slower, as it would be in the small x_F region. At large x_F the J/ψ shows an increasingly strong suppression. Two different models claim to explain this effect. One is the intrinsic charm model of Brodsky, which was mentioned earlier in this talk. The other is a simpler model from Gavin¹⁸ which explains this behavior as resulting from energy loss effects in both the incident and final state. The basic idea behind this model can be understood in simple terms by considering the x_F distribution of the production process which is depicted schematically in Fig. 9. When one goes from deuterium to a heavy nucleus the additional energy loss can shift the effective x_F distribution towards smaller x_F resulting in a ratio which falls with larger x_F as shown. A similar but smaller effect in the DY x_F dependence resulting from only the initial state is also explained within this model.

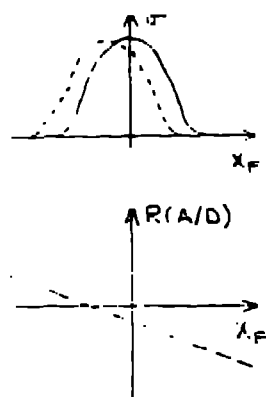


Fig. 9. Cartoon picture of how a shift in the x_F distribution affects the ratio.

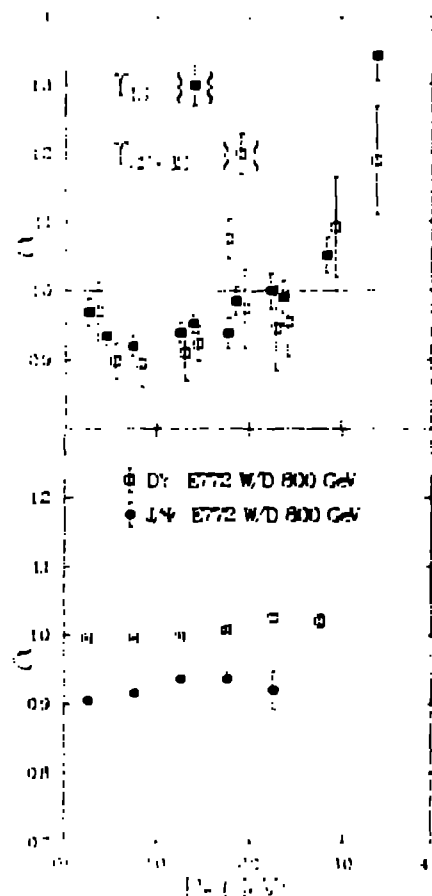


Fig. 10. p_T -dependence for J/ψ and Υ production from E772.

The p_T dependence of α for resonance production is shown in Fig. 10. DY and J/ψ production show a similar increase of α as p_T increases presumably caused, at least in part, by initial-state multiple scattering effects. Similar results have been reported by NA38¹⁹ where they show that multiple scattering effects can explain both proton-nucleus and nucleus-nucleus J/ψ production p_T dependences. Although the overall trend for our data on Υ production is similar to that of our J/ψ data the shape is quite different with increases both at very small p_T and for large p_T . At this time I do not know of any explanation for this dramatic difference for Υ production.

J/ψ suppression has also been observed in heavy ion collisions. Yields of J/ψ relative to the Drell Yan background are reduced in central collisions relative to peripheral collisions. Central collisions, which correspond to small impact parameter, are presumed

to be able to create quark-gluon plasma for which such a suppression was predicted.²⁰ However it is clear that whatever effects are responsible for the suppression of proton-nucleus J/ψ production may also play an important role in heavy-ion J/ψ production and could explain most of the suppression seen with heavy-ions. Detailed comparisons have been done in Refs.^{11,17}

E789 is now running at Fermilab. One of the goals of this run is to determine the A-dependence of D production and to compare to the results already obtained for J/ψ and Υ production. The standard mechanism for loss of J/ψ 's due to interaction of a pre- J/ψ with either the nucleus or comovers is dissociation into a $D\bar{D}$ pair. In this case the loss of J/ψ 's would apparently feed the production of D 's, tending to enhance D production. However recent data from WA82 for D -meson production suggests that the A-dependence for D 's may be even stronger than that for the J/ψ .²¹ If this is true then it may be inconsistent to describe the main mechanism for suppression of J/ψ production as dissociation to $D\bar{D}$ pairs.

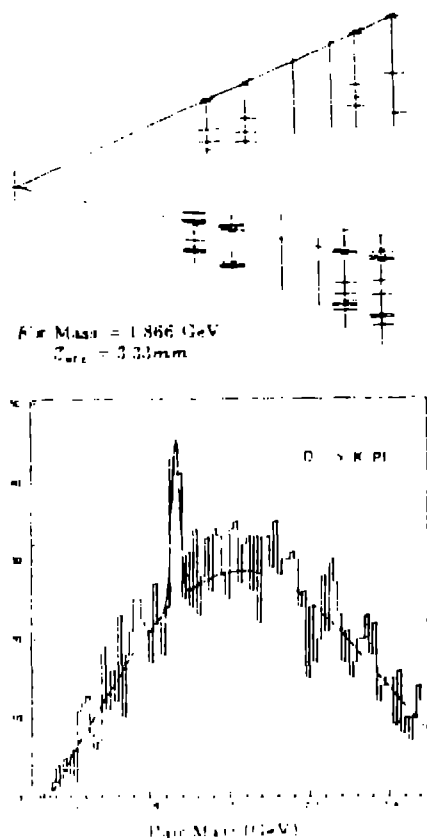


Fig. 11. A $D \rightarrow K\pi$ event seen in the 8-plane silicon vertex detector used during our 1990 test run and the mass peak corresponding to downstream decays of the D also from the test run

As part of the upgrade of our spectrometer for E789 we have installed a 16-plane silicon multi-strip vertex detector just downstream of our experimental target. This vertex detector can locate the vertex of the detected decay particles (e.g. $D^0 \rightarrow K^+ \pi^-$) to better than a millimeter in Z . Since the average decay distance of a D is about 3 mm, and with a very thin target, D 's can be identified by their downstream decays with a typical efficiency of 30% and a prompt target dihadron rejection of 10^4 or better. An example of a prompt downstream D decay reconstructed in the silicon vertex detector obtained during our 1990 test run is shown in Fig. 11 along with an invariant mass spectrum with a clear peak at the D mass of 1.86 GeV. During the test run only 8 planes of silicon were operational. The new data being taken now with 16 planes of silicon will

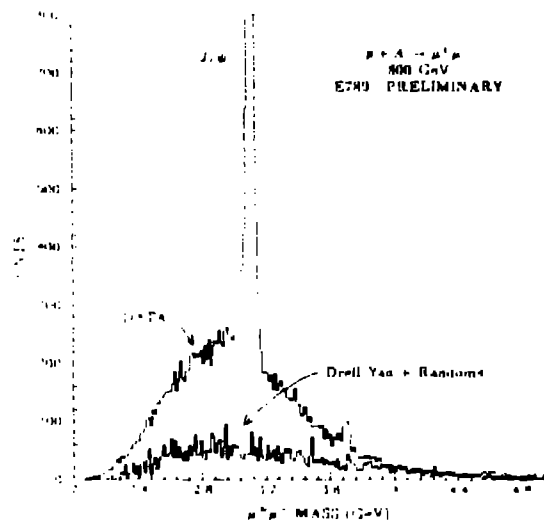


Fig. 12. The di-muon mass spectrum in the region of the J/ψ showing the predicted Drell-Yan + random contribution. The region below the J/ψ in mass is apparently dominated by semi-leptonic decays of charm.

have correspondingly better efficiency for downstream decays and rejection of target backgrounds. Our estimate is that we already have approximately 7000 reconstructable D 's on tape (including efficiency losses) of which about 700 are from the Be target and the rest from W . However it will take some time before we have our offline tracking tuned up adequately for the new silicon configuration and are able to produce new results including the A -dependence.

Another issue that our new data addresses is the content of the continuum in the mass region below the J/ψ . This is one of the regions where a signal from the quark-gluon plasma could be evident. Preliminary results from our recent measurements, as shown in Fig. 12, indicate that this region is dominated by charm. Calculations of the DY contribution, although somewhat unreliable in the mass region, show that the DY contribution is negligible compared to our data. The charm contribution, which comes from decay of a correlated $D-\bar{D}$ pair into di-leptons via semi-leptonic decays, can be directly determined by measuring the $\mu^\pm e^\mp$ mass spectrum. We have done this and find that essentially all the continuum in the 2 to 3 GeV region can be explained by charm. The contribution from randoms in our experiment was found to be negligible. These conclusions are based on a very recent analysis of a very small portion of our data and will become more definitive as our analysis progresses. However it is already clear that signatures of quark-gluon plasma via continuum di-leptons in the 2 to 3 GeV mass region will be overwhelmed by charm decays.

VII. Summary

Precise measurements of the A -dependence of the Drell-Yan and of resonance (J/ψ , ψ' , Υ) production have been made in Fermilab E772 and E789. The anti-quark structure function is not affected by the nuclear medium up to $x \leq 0.3$ except in the shadowing region at very small x ($x \leq 0.1$). Models which produce a significant anti-quark enhancement or depletion for $0.1 \leq x \leq 0.3$ are ruled out. Vector meson production of J/ψ , ψ' , and Υ all exhibit a large suppression in a heavy nucleus with the strongest suppression for the J/ψ and ψ' . This suppression is strongest for large x_F and for x_F at or below zero. The integrated A -dependence yields an α of .92 for the J/ψ and ψ' and .96 for the Υ 's. It is not clear how to decouple structure and reaction mechanism effects in order to extract the A -dependence of the gluon structure function. The p_T distribution is broadened for the J/ψ presumably due to initial-state effects. For the Υ a more dramatic and complicated p_T dependence is seen for which no simple explanation is known. J/ψ suppression in proton-nucleus and in heavy-ion collisions probably share common physical origins (e.g. initial and final-state effects). Thus a clear understanding of proton-nucleus vector-meson production including more comprehensive data will be essential in order to understand production in heavy-ion collisions and to look for effects of a quark-gluon plasma.

References

- ¹M. Ericson and A. W. Thomas, Phys. Lett. 128B (1983) 112.
- ²R. P. Bickerstaff, M. C. Birse, and G. A. Miller, Phys. Rev. Lett. 53 (1984) 2532.
- ³E. L. Berger, F. Coester, and R. B. Wiringa, Phys. Rev. D29 (1984) 398.
- ⁴F. E. Close, R. G. Roberts, and G. G. Ross, Phys. Lett. 129B (1983) 346.
- ⁵R. L. Jaffee, Phys. Rev. Lett. 50 (1983) 228.
- ⁶F. E. Close, R. L. Jaffee, R. G. Roberts, and G. G. Ross, Phys. Rev. D31 (1985) 1004.
- ⁷C. E. Carlson and T. J. Havens, Phys. Rev. Lett. 51 (1983) 261.
- ⁸Hans J. Pirner and James P. Vary, Phys. Rev. Lett. 46 (1981) 1376.
- ⁹N. N. Nicolaev and V. I. Zakharov, Phys. Lett. B55 (1975) 397; A. H. Mueller and J. Qiu, Nucl. Phys. B268 (1986) 427; and Edmond L. Berger and Jianwei Qiu, Phys. Lett. B141 (1988) 119.
- ¹⁰Stanley J. Brodsky and Hung Jung Lu, Phys. Rev. Lett. 64 (1990) 1342.
- ¹¹S. Gavin and R. Vogt, Nucl. Phys. B345 (1990) 104.
- ¹²Stanley J. Brodsky and Paul Hoyer, Phys. Rev. Lett. 63, (1989) 1566.
- ¹³D. M. Alde, *et al.*, Phys. Rev. Lett. 64 (1990) 2479; Phys. Rev. Lett. 66 (1991) 133; and Phys. Rev. Lett. 66 (1991) 2285.
- ¹⁴G. Altarelli, R. K. Ellis, and G. Martinelli, Nucl. Phys. B157 (1979) 461; J. C. Collins, D. E. Soper, and G. Sterman, Phys. Lett. 134B (1984) 263; and I. R. Kenyon, Rep. Prog. Phys. 45 (1982) 1261.
- ¹⁵J. J. Aubert, *et al.*, Phys. Lett. B123 (1983) 275; and J. Ashman, *et al.*, Phys. Lett. B202 (1988) 603.
- ¹⁶W. Y. P. Hwang, J. M. Moss, and J. C. Peng, Phys. Rev. D38 (1988) 2785.
- ¹⁷R. Vogt, S. J. Brodsky, and P. Hoyer, Nucl. Phys. B360 (1991) 67.; and S. J. Brodsky and R. Vogt, private communication.
- ¹⁸S. Gavin and J. Milana. William and Mary preprint WM-91-116.
- ¹⁹C. Baglin, *et al.*, Phys. Lett. B220 (1989) 471; and Phys. Lett. B268, (1991) 453.
- ²⁰T. Matsui and H. Satz, Phys. Lett. B178 (1986) 416.
- ²¹A. Forino, *et al.* (WA82) preprint.